Infection and Drug Resistance

Dovepress
Taylor & Francis Group

Open Access Full Text Article

ORIGINAL RESEARCH

Divergent Virulence Traits in *Klebsiella Pneumoniae* Strains of Capsular Serotype K2 and ST25: Insights from Whole-Genome Sequencing

Qingqing Du[1–3,*], Fen Pan[1–3,*], Fangyuan Yu[1–3], Jie Jiang[1–3], Chun Wang[1–3], Huihong Qin[1–3], Wenxin Liu[1–3], Xiaozhou Pan[1–3], Zhan Ma[1–3], Wenhao Weng[1–3], Dingding Han[1–3], Hong Zhang[1–3]

[1]Department of Clinical Laboratory, Shanghai Children's Hospital, School of Medicine, Shanghai Jiao Tong University, Shanghai, People's Republic of China; [2]Institute of Pediatric Infection, Immunity, and Critical Care Medicine, Shanghai Jiao Tong University School of Medicine, Shanghai, People's Republic of China; [3]College of Health Science and Technology, Shanghai Jiao Tong University School of Medicine, Shanghai, People's Republic of China

*These authors contributed equally to this work

Correspondence: Dingding Han; Hong Zhang, Email handingding517@hotmail.com; schjyk2015@126.com

Abstract: Hypervirulent *Klebsiella pneumoniae* (hvKp) poses significant challenges for clinicians, yet the virulence determinants of hvKp have not been fully ascertained. In our study, we observed a divergence in virulence between two K2-ST25 *Klebsiella pneumoniae* strains, both of which carried the *rmpA, iroB* and *peg344* virulence-associated genes. These strains exhibited different median death time (12 hour *vs* over one week in BALB/c) in the mice lethality assay. Whole genome sequencing (WGS) revealed that the virulence plasmids of hvKp CHK014 and non-hvKp CHK036, namely pCHK014 and pCHK036-1, shared 99.92% and 95.92% identity with the classic hypervirulent plasmid pLVPK, respectively. Additionally, in non-hvKp CHK036, the *rmpA* gene, along with the *iro* operon, *iutA* gene and *peg344* gene, was located in the integrative and conjugative element ICE*Kp1* in the chromosome. However, in hvKp CHK014, the *rmpA* gene, *peg344* gene and the *iro* operon were located on the IncFIB/IncHI3B virulence plasmid. Furthermore, RT-qPCR results demonstrated significantly higher expression levels of the *rmpA, iroB* and *peg344* genes in hvKp CHK014 compared to non-hvKp CHK036. Correspondingly, the capsular polysaccharide yields regulated by the *rmpA* gene were significantly higher in CHK014 than CHK036. Although the copy number of *rmpA* gene in both strains was not altered, the poly (T) track on *rmpA* promoter remains as P_{11T}, which contributed to the elevated expression level in hvKp CHK014. Whereas the poly(T) track on *rmpA* promoter in non-hvKp CHK036 was P_{10T}, a shorten form of poly(T). Meanwhile, the promotor of *rmpA* on CHK036 included 38 additional variants, compared with CHK014 and pLVPK. These findings indicated that the expression of the *rmpA* gene was a crucial virulence determinant, with the P_{11T} on promoter of *rmpA* gene having a higher expression potential and thus contributing to the virulence difference between hvKp CHK014 and non-hvKp CHK036 in our murine infection model.

Keywords: *Klebsiella pneumoniae*, hypervirulence, whole-genome sequencing, gene promotor

Introduction

Klebsiella pneumoniae is a major clinical Gram-negative pathogen that commonly causes nosocomial and healthcare-associated infections including pneumonia, abscess, bacteremia, and urinary tract infections. In particular, hypervirulent *K. pneumoniae* (hvKp), initially identified from patients with liver abscess in Taiwan in the late 1980s, is capable of causing life-threatening infections such as pyogenic liver abscesses, endophthalmitis, septicemia and meningitis in healthy individuals. Compared to classic *K. pneumoniae* (cKp), hvKp has a higher capacity to effectively acquire iron and produce larger amounts of capsular polysaccharides (CPS), which confers *K pneumoniae* a hypermucoviscous phenotype in the string test as generating viscous strings >5 mm in length when a loop stretches the colony on an agar plate.[1] The hypermucoviscous phenotype is considered to be mediated by a pLVPK-like virulence plasmid carrying two

https://doi.org/10.2147/IDR.S573797
Received: 12 October 2025
Accepted: 30 December 2025
Published: 29 January 2026

polysaccharide regulator genes (*rmpA*/*A2*) and several siderophore determinants (aerobactin biosynthetic genes *iucABCD-iutA* and salmochelin biosynthetic genes *iroBCDN*).[2,3]

Epidemiological studies have identified high-risk clones of hvKp, such as capsular serotype K1- sequence type 23 (ST23) and capsular serotype K2-ST86/ST65/ST375.[4,5] Recently, a novel high-risk clone, K2-ST25 hvKp, has been increasingly reported worldwide[6,7] since its initial detection in 2008 in Vietnam and Laos.[8] This emerging clone poses a potential public health threat as it can cause severe systemic disease in diverse patient populations, including liver abscess with endogenous endophthalmitis in adults[9] and septicaemia outbreaks in pigs.[10,11] The coexistence of virulence and resistance traits underscores the strong risk potential of K2-ST25, posing serious challenges for clinical management and infection control.[12,13] Furthermore, a recent study highlighted the divergence in virulence and innate immune response in a murine model between two *K. pneumoniae* ST25 strains, both carrying enterobactin-encoding genes and salmochelin-encoding genes.[14] However, the underlying reason for the varying virulence levels among these ST25 strains with similar virulence factors remains unclear.

Between 2019 and 2020, we examined 352 isolates using genetic biomarkers (*rmpA*/*A2, iucA, iroB, peg344*[15]) for surveillance of hvKp. During this period, we identified six K2-ST25 carrying hypervirulence genes *K. pneumoniae*. Notably, in the half-year interval from July 2019 to January 2020, there was an outbreak of four cases infected by K2-ST25 clonotype *K. pneumoniae* in neonatal wards. These cases prompted further investigation into the virulence potential of K2-ST25 strains both in vivo and in vitro. Our study aimed to elucidate the virulence divergence of the K2-ST25 clone. Through whole-genome sequencing and functional experiments, we identified the determinants responsible for the hypervirulence of the newly emerging K2-ST25 *K. pneumoniae* in vivo and in vitro.

Materials and Methods

Bacterial Isolates and Virulence Determination

Consecutive and nonrepetitive clinical *K. pneumoniae* isolates were collected and stored at Shanghai Children's Hospital from January 2019 to December 2020, as previously described.[16] HvKp was defined by the presence of at least one virulence-associated genetic marker (*rmpA*/*rmpA*2/*iucA*/*iroB*/*peg344*),[15] along with the high lethality in *Galleria mellonella* and at least one other hypervirulence phenotype (hypermucoviscosity/serum resistance/excessive siderophore production). Virulence phenotypic assays, including the string test, serum killing assay, relative quantitative siderophore production assay and mouse lethality assays, as well as standard PCR for screening carbapenemase genes, extended-spectrum β-lactamase (ESBL) genes, virulence-associated genes, capsule typing and multilocus sequence typing (MLST) were detailed in our previous study.[16] Prior to surgery and antimicrobial treatment, the hvKp CHK014 strain was isolated from a sputum sample of a 1-month-old critically ill female patient. On the other hand, the non-hvKp CHK036 strain was isolated from a urine sample of a 4-month-old male patient with a favorable prognosis.

Antimicrobial Susceptibility Testing

Antimicrobial susceptibility was confirmed utilizing the Kirby-Bauer disk and VITEK 2 system tests. The susceptibility results were interpreted following the CLSI guidelines.[17] The in vitro activity of tigecycline was assessed according to FDA standards,[18] while the in vitro activity of polymyxin B was determined based on thresholds set by the European Committee on Antimicrobial Susceptibility Testing.[19] *Escherichia coli* ATCC 25922 served as the quality control strain.

Multi-drug resistance was defined as non-susceptibility to at least one agent in three or more antimicrobial categories, according to Magiorakos et al's definition.[20]

Whole Genome Sequencing and Analysis

Genomic DNA from two selected strains, hvKp CHK014 and non-hvKp CHK036, was extracted and subjected to whole-genome sequencing. The sequencing was performed using the PacBio Sequel single-molecule real-time sequencing and Illumina NovaSeq sequencing platforms (paired-end, 2 by 150 bp). Raw reads were de novo assembled with HGAP and CANU softwares, then refined with Pilon software. Annotation of the assembled sequences was carried out using the RAST tool (https://rast.nmpdr.org/) and the NCBI PGAP (http://www.ncbi.nlm.nih.gov/genome/annotation_prok). The

sequence types (STs) were determined with a database available at http://bigsdb.pasteur.fr/klebsiella/klebsiella.html. Capsular typing was performed using Kaptive (https://github.com/katholt/Kleborate/). Molecular function and network of protein-encoding genes were annotated using Gene Ontology (GO) and Kyoto Encyclopedia of Genes and Genomes (KEGG) database. Virulence genes were identified using the virulence factor database (VFDB), and resistance genes were identified using the comprehensive antibiotic resistance database (CARD) (https://card.mcmaster.ca/) and the Resfinder database (https://cge.cbs.dtu.dk/services/). Plasmid replicons were identified using KpVR (https://bioinfo-mml.sjtu.edu.cn/KpVR/index.php). The origin of transfers in DNA sequences of bacterial mobile genetic elements was identified using oriTfinder (https://tool-mml.sjtu.edu.cn/oriTfinder/oriTfinder.html), Integrative and conjugative elements (ICEs) were detected by ICEfinder (https://bioinfo-mml.sjtu.edu.cn/ICEfinder/ICEfinder.html) and Insertion elements (IS) were identified by IS Finder (http://integrall.bio.ua.pt/).

Quantitative Analysis of Virulence Genes

The quantitative analysis of *rmpA, iroB* and *peg344* genes (the primers listed in Table S1) was conducted using reverse transcriptase-quantitative PCR (RT-qPCR).[21] The *rho* gene was used as the reference gene. Bacterial strains were cultured in LB medium at 37 °C, with cells harvested during the exponential phase of growth. Total RNA was extracted using the RNAprep pure cell/bacteria kit (TIANGEN), followed by DNase I treatment using a ReverTra Ace qPCR RT Master Mix with gDNA Remover (TOYOBO) to remove contaminating DNA. RNA concentration and quality were assessed by measuring the absorbance at 260 nm. RT-PCR was carried out using SYBR® Green Realtime PCR Master Mix (TOYOBO). The experiments were conducted in triplicate and repeated three times. The relative transcript expression was determined by calculating differences in the comparative cycle threshold (Ct) method.[22]

Bacterial Growth Analysis

The growth curve of bacterial strains was detected following the method described before.[23] Briefly, overnight cultures were diluted 1:1000 in 30 mL of fresh LB medium, and incubated at 37°C with continuous shaking at 200 rpm. The cell density was measured every 1 or 2 hours by measuring the optical density at 600 nm (OD_{600}).

Biofilm Production Assay

The ability of selected *K. pneumoniae* strains to form biofilms was evaluated following a previously established protocol.[24] Overnight bacterial cultures were resuspended in LB broth at a concentration of 0.5 McFarland and then diluted 1:100. The diluted cultures were transferred to 96-well plates containing 200 μL of LB medium. After incubation for 24 hours at 37°C, the supernatant was removed and each well was washed three times with PBS. The organisms in the wells were stained with 1% crystal violet for 30 minutes at room temperature, and the excess stain was washed off with slow-running water. The stained biofilm was then solubilized with 200 μL of absolute alcohol and the absorbance at 590 nm was measured to quantify the biofilm formation. The assay was performed in triplicate.

Capsule Production Assay

The CPS of *K. pneumoniae* strains were purified following the previously described method.[25] Overnight cultures of *K. pneumoniae* strains (1×10^9 CFU) were centrifuged, resuspended in 500 μL of PBS. The bacterial cells were then mixed with 200 μL of 1% Zwittergent (Sangon Biotech) in 100 mM citric acid buffer (Sangon Biotech) at 55°C for 30 min. After centrifugation at 10000 g for 10 min, 0.4 mL of the cell-free supernatant was combined with 1.6 mL of absolute ethanol and incubated for 30 min at 4°C. The samples were then centrifuged, rehydrated with 125 μL of water overnight, and mixed with 0.5 mL of 12.5 mM sodium tetraborate (Sigma) in concentrated sulfuric acid (Sinopharm). The concentration of uronic acid were determined using a standard curve of glucuronic acid (Sangon Biotech).[26]

Siderophore Production Assay

In the qualitative plate siderophore production assay, 3 mL of stationary-phase iron-chelated cultures were dropped onto modified King B agar plates containing chrome azurol S dye (CAS) solution (Coolaber). Siderophore production was

confirmed by the presence of opaque golden-yellow halos after overnight incubation at 37°C.[15] Positive and negative controls, NTUH-K2044 and a cKp strain, respectively, were included. Each assay was conducted in triplicate.

For the relatively quantitative solution-based siderophore production assay, a colony of each strain was inoculated into iron-chelated M9 minimal medium containing Casamino Acids (c-M9-CA) and grown overnight at 37°C with shaking at 180 rpm.[27] Then, 100 μL supernatant from each bacterial suspension was diluted 5-fold in c-M9-CA and added to 100 μL CAS solution (Coolaber) in a flat-bottom 96-well plate. After incubation in the dark for 30 min, the absorbance was measured at A630 nm. c-M9-CA plus CAS solution was used as a reference (r). Siderophore units (Su) were calculated using the formula: [(Ar - As)/Ar] × 100%. Each assay was performed in duplicate and repeated twice independently.

Murine Infection Model

Mouse lethality assays were conducted on 5-week-old male BALB/c mice (mean weight, approximately 16 g) obtained from Shanghai JieSiJie Laboratory Animal Co., Ltd. (Shanghai, China). Each isolate was intraperitoneally administered to five mice per group at a bacterial concentration of 1×10^6 CFU. The sample size was estimated using 90% of power at an alpha level of 0.5 (https://www.bu.edu/researchsupport/compliance/animal-care/working-with-animals/research/sample-size-calculations-iacuc/). Mice were randomly allocated by the RANDBETWEEN function in the Excel software according to their index number, so potential confounders were inevitable system error. During group allocation, conduct of the experiment, outcome assessment, and data analysis, we followed the principle of double-blind. Mortality of the mice was monitored over a 7-day period. Following the demise of a mouse, its organs (heart, liver, lungs, and kidneys) were aseptically collected within 12 hours. Organ sections were fixed in paraformaldehyde and embedded in paraffin. Subsequently, H&E and Gram staining were performed on the sections to assess areas of bleeding. Four different views of each section were examined to evaluate bleeding areas, using ImageJ software (National Institutes of Health, USA). NTUH-K2044 and cKp were served as hypervirulent and low-virulent controls, respectively.

Statistical Analysis

GraphPad Software version 8.4.3 was employed for data analysis. Unpaired *t*-test or Mann–Whitney *U*-test was used for continuous variables, while Chi-square test or Fisher's exact test was employed for categorical variables. Statistical significance was determined for *P*-values less than 0.05.

Ethics Statement

This retrospective study was approved by the Shanghai Children's Hospital Institutional Review Board (2022R059-E01). The clinical samples were residual specimens collected during routine hospital laboratory procedures for diagnostic purposes. All animal procedures in this study were performed in accordance with guidelines for the ethical review of laboratory animal welfare People's Republic of China National Standard GB/T 35892–2018 and approved by the Shanghai Children's Hospital Ethics Committee. Clinical trial number: Not applicable.

Results

Outbreak of K2-ST25 Hypervirulent K. Pneumoniae in the Neonatal Unit

Between 2019 and 2020, our epidemiological investigation on the prevalence of *K. pneumoniae* among children in a tertiary hospital in Shanghai revealed that the predominant clones of hypervirulent *K. pneumoniae* were K1-ST23 and K2-ST25, indicating that K2-ST25 was a high-risk clone with both hypervirulence and nosocomial transmissibility. Notably, all three cases of K2-ST25 hvKp infection were identified in the neonatal unit from July 2019 to November 2020. Importantly, three other *K. pneumoniae* isolates carrying virulence-associated genes exhibited a low virulence phenotype (Table 1).

Virulence Divergence in K2-ST25 Klebsiella Pneumoniae

It was found that while non-hvKp strain 2 (CHK036) and non-hvKp strain 3 infections resulted in similar lethality in *G. mellonella* as hvKp, they did not display other hypervirulent traits (hypermucoviscousity/serum resistance/excessive

Table 1 Characterization Survey of K2-ST25 hvKp Isolates (n = 3) and Non-hvKp with Virulence-Associated Genes (n = 3)

Strains	Isolation Date	Source of Isolates (Wards)	Recovery Sites (Specimen)	Virulence-Associated Genes	Resistance Genes	Median Lethal Time of Mice[a]	24-Hour Lethality of *G. mellonella*	String Test	Serum Resistance (Grade)	Siderophore Production
HvKp 1 (2019K134[16])	Jul. 2019	Neonatal	Sputum	*rmpA-iroB-peg344*	bla_{SHV}-bla_{CTX}, bla_{DHA}-bla_{EBC}	12h	50%	Postive	6	6.85%
HvKp 2 (2019K164[16])	Aug. 2019	Neonatal	Sputum	*rmpA-iroB-peg344*	bla_{SHV}	Not tested	70%	Negative	5	0.73%
HvKp 3 (CHK014 in this study; 2020K14[16])	Jan. 2020	Neonatal	Sputum	*rmpA-iroB-peg344*	bla_{SHV}	12h	90%	Postive	5	0.13%
Non-hvKp 1 (2019K139[16])	Jul. 2019	Neonatal	Sputum	*rmpA-iroB*	bla_{SHV}-bla_{CTX}- bla_{TEM}	Not tested	10%	Negative	4	16.98%
Non-hvKp 2 (CHK036 in this study; 2020K36[16])	Apr. 2020	Emergence	Urine	*rmpA-iucA-iroB-peg344*	bla_{SHV}-bla_{CTX}- bla_{TEM}	Over 7 days	70%	Negative	4	16.83%
Non-hvKp 3 (2020K51[16])	May. 2020	Nephrology	Urine	*rmpA-iucA-iroB-peg344*	bla_{SHV}	Not tested	60%	Negative	4	23.09%

Notes: [a]We randomly selected three K2-ST25 strains to perform mouse lethality assay by using the RANDBETWEEN function in the Excel software, so potential confounders were inevitable system error. During group allocation, conduct of the experiment, outcome assessment, and data analysis, we followed the principle of double-blind.

https://doi.org/10.2147/IDR.S573797

siderophore production).[16] Mice infected with the non-hvKp CHK036 strain had a significantly higher overall survival rate compared to those infected with the hvKp CHK014 strain (Table 1). Furthermore, hvKp CHK014-infected mice showed significantly notably increased bleeding areas in the liver ($P = 0.0286$) and kidney ($P = 0.0286$) compared to non-hvKp CHK036-infected mice. Additionally, there is much more obvious interstitial vascular congestion, edema, inflammatory cells infiltration in hvKP-infected mice than that in non-hvKP-infected mice (Figure 1). The bacterial burdens in organs were also higher in mice infected with hvKp CHK014 (10^8–10^10 CFU/g) than in those infected with non-hvKp CHK036 (10^4–10^6 CFU/g) (Figure 2). These results indicated varying levels of virulence between two K2-ST25 *Klebsiella pneumoniae* isolates with CHK014 being relatively more virulent and more resistant to clearance by the immune system clearance during murine systemic infection.

The CHK036 isolate was resistant to multiple antimicrobials including ceftriaxone, cefazolin, cefuroxime, cefotaxime, cefepime, ceftazidime and trimethoprim-sulfamethoxazole, whereas the CHK014 isolate was only resistant to cefuroxime and cefoxitin among the tested antimicrobials.

Virulence-Associated Phenotypes Differences Between hvKp CHK014 and Non-hvKp CHK036

Various phenotypic assays were conducted to assess the in-vitro virulence of hvKp CHK014 and non-hvKp CHK036. It was observed that the growth rate of hvKp CHK014 was significantly lower compared to the non-hvKp CHK036 ($P = 0.0214$; Figure 3A). However, there was no significant difference in biofilm production between the two isolates ($P =$

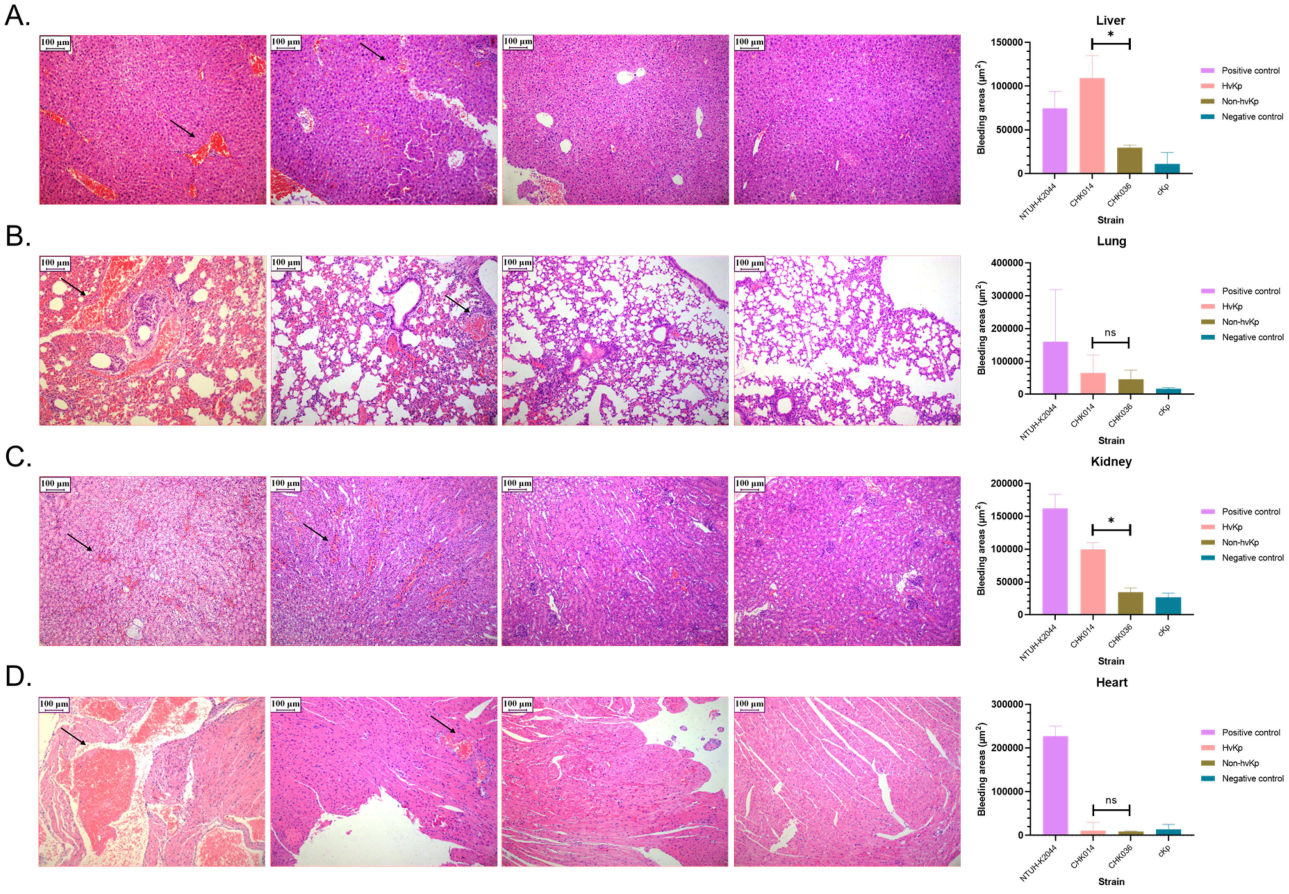

Figure 1 Damage of hvKp infection to mice. Histological changes in livers (**A**) lungs (**B**) kidneys (**C**) and hearts (**D**) of infected mice. From left to right, images show mouse organs infected with NTUH-K2044, hvKp CHK014, non-hvKp CHK036, and cKp, respectively. Black arrows indicate areas of hemorrhage within the tissues. Data of organs bleeding areas were expressed as medians with interquartile ranges, $P < 0.05$ (*) and $P > 0.05$ (ns). Between CHK014 and CHK036 isolates infected mice, significant differences were observed in the bleeding areas of liver ($P = 0.0286$), and of kidney ($P = 0.0286$), but not of lung ($P > 0.9999$) and heart ($P = 0.6857$) using Mann–Whitney test.

https://doi.org/10.2147/IDR.S573797

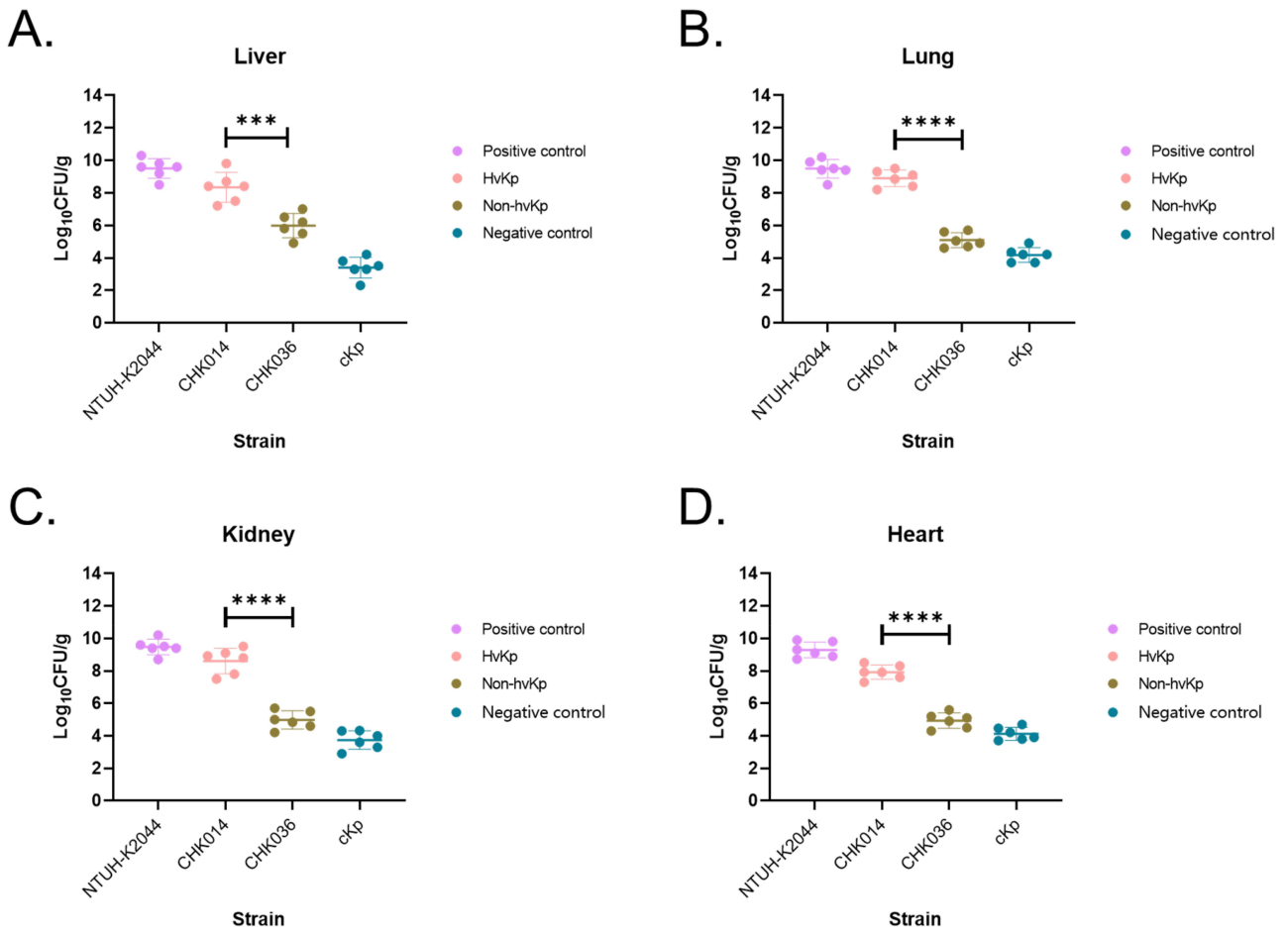

Figure 2 Bacterial burdens in livers (**A**) lungs (**B**) kidneys (**C**) and hearts (**D**) of infected mice. Data shown are means ± SDs, $P < 0.001$ (***), $P < 0.0001$ (****). Between hvKp CHK014 and non-hvKp CHK036 isolates infected mice, significant differences were observed in bacterial CFU of liver (t = 4.844, $P = 0.0007$, 95% confidence interval [CI] = −3.431 to −1.269), of lung (t = 13.54, $P < 0.0001$, 95% CI = −4.427 to −3.176), of kidney (t = 9.258, $P < 0.0001$, 95% CI = −4.505 to −2.757), and of heart (t = 11.28, $P < 0.0001$, 95% CI = −3.576 to −2.396) using unpaired *t*-test.

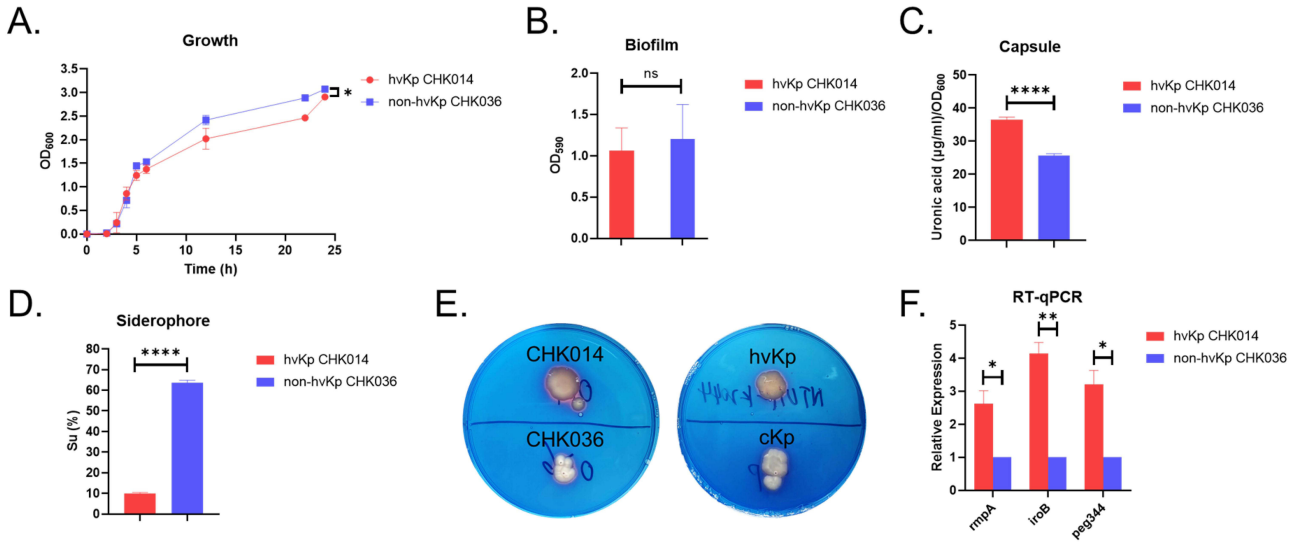

Figure 3 Virulence phenotypes of hvKp CHK014 and non-hvKp CHK036. Growth analysis (**A**) biofilm production (**B**) capsule production (**C**) relative quantitative siderophore production (**D**), qualitative siderophore production (**E**), and quantitative analysis of *rmpA*, *iroB* and *peg344* genes (**F**) of CHK014 and CHK036. $P < 0.05$ (*), $P < 0.01$ (**), $P < 0.0001$ (****) and $P > 0.05$ (ns). Between hvKp CHK014 and non-hvKp CHK036 isolates, significant differences were observed in growth rate ($P = 0.0214$), CPS yield ($P < 0.0001$), qualitative siderophore production ($P < 0.0001$), and in the expression levels of *rmpA* ($P = 0.0192$), *iroB* ($P = 0.0037$), and *peg344* ($P = 0.0118$) genes. No significant difference was observed in biofilm production ($P = 0.6654$).

https://doi.org/10.2147/IDR.S573797

0.6654; Figure 3B). CPS yields regulated by the *rmpA* gene were significantly higher in CHK014 compared to CHK036 ($P < 0.0001$; Figure 3C). Regarding siderophore production regulated by *iuc* and *iro* lineage, quantitative assay showed significantly lower siderophore production in CHK014 than that in CHK036 (Figure 3D), but qualitative plate assay showed CHK014 appeared more obvious orange halos on siderophore plates than CHK036 ($P < 0.0001$; Figure 3E). To understand the virulence difference between hvKp CHK014 and non-hvKp CHK036, we examined the expression levels of *rmpA, iroB*, and *peg344* genes. RT-qPCR results demonstrated significantly higher expression levels of *rmpA* ($P = 0.0192$), *iroB* ($P = 0.0037$), and *peg344* ($P = 0.0118$) genes in hvKp CHK014 compared to non-hvKp CHK036 (Figure 3F).

Genomic Characterization of hvKp CHK014 and Non-hvKp CHK036

To investigate the genomic contribution to the expression divergence in specific virulence genes of K2-ST25 *Klebsiella pneumoniae*, whole genome sequencing was conducted on hvKp CHK014 and non-hvKp CHK036 (GenBank BioProject accession number: PRJNA1015570).

The hvKp CHK014 genome comprised a single chromosome of 5,268,439 bp (57.57% GC content, Open Reading Frames (ORFs) length 4,565,898 bp) with 109 antimicrobial resistance genes and 74 virulence genes, and one plasmid, pCHK014 (193,013 bp, 50.25% GC content, ORFs length 158,667 bp) with one antimicrobial resistance gene and 14 virulence genes. On the other hand, the non-hvKp CHK036 genome consisted of a single chromosome of 5,346,405 bp (57.54% GC content, ORFs length 4,630,479 bp) with 109 antimicrobial resistance genes, and three plasmids: pCHK036-1 (195,446 bp, 51.81% GC content, ORFs length 154,518 bp) with one antimicrobial resistance gene and 11 virulence genes, pCHK036-2 (109,636 bp, 48.99% GC content, ORFs length 94,773 bp) without virulence or antimicrobial resistance genes, and pCHK036-3 (94,151 bp, 52.50% GC content, ORFs length 72,993 bp) with 17 antimicrobial resistance genes but lacking virulence genes (Table S2). Neither CHK014 nor CHK036 harbored any carbapenemase genes. Multilocus sequence typing and capsular *wzi* allele typing confirmed that both strains belonged to the K2-ST25 subclone.

Out of the 5,493 genes in CHK036 and 5,161 genes in CHK014, 4,579 genes were categorized as orthologs gene families, with 231 gene families unique to CHK014 and 566 gene families unique to CHK036 (Figure S1A). Further analyses through GO and KEGG indicated that these unique genes were predominantly associated with signal transduction and cell transformation activities (Figures S1B, S1C and Table S3).

Genomic Insights into the Virulence Diversity of hvKp CHK014 and Non-hvKp CHK036

Previous PCR screening results showed that hvKp CHK014 was positive for the virulence-associated genes *rmpA, iroB*, and *peg344*, while non-hvKp CHK036 was positive for *rmpA, iucA, iroB* and *peg344*. WGS confirmed the presence of *rmpA, iroB* and *peg344* in CHK014, and *rmpA, iucA, iroB* and *peg344* in CHK036.

WGS data further revealed that in non-hvKp CHK036, the gene cluster *iucABCD-iutA* was located in the IncFIB/IncFII conjugative virulence plasmid pCHK036-1. Additionally, *rmpA-rmpD-rmpC, iroD-iroC-iroB-iroN* operon, *peg344* gene, and another *iutA* gene copy were located in the ICE*Kp1* (63,457 bp) element of the chromosome, indicating the presence of the *iutA* gene on both the chromosome and the virulence plasmid. The 63.4-kb DNA fragment ICE*Kp1* was positioned near the 3′-end of an *asn*-tRNA gene and was flanked by 15-bp direct repeats (TGCGCCAGTGCGAGC). Apart from ICE*Kp1*, six other ICE variants encoding prophage core component proteins were identified in the chromosome. In contrast to the typical ICE*Kp1* (GenBank accession numbers AB298504), the genetic context of the *iro* lineage on CHK036 displayed *iroD, iroC* and *iroB*, and the *iroN* gene in order at a ~2 Mb interval from the other three genes. In hvKp CHK014, the nonconjugative IncFIB/IncHI3B virulence plasmid pCHK014 carried *rmpA-rmpD-rmpC* genes, *peg344* gene and *iroN-iroD-iroC-iroB* operon (with *rmpADC* and *peg344* genes located upstream of the *iro* lineage), but did not contain the *iutA* gene or *iuc* lineage.

To investigate the genomic heterogeneity in the virulence potential of K2-ST25 *K. pneumoniae*, we conducted a comparative analysis of the complete genomic sequences of two virulence plasmids, pCHK014 and pCHK036-1,

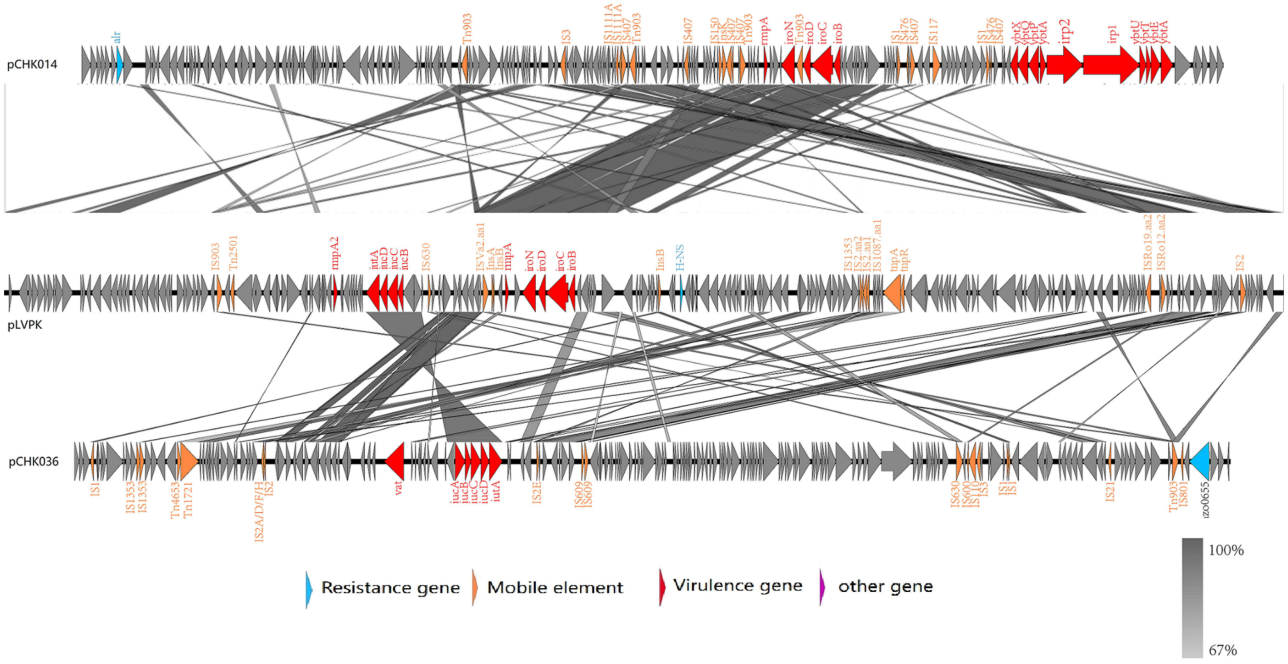

Figure 4 Comparative analysis of pCHK014 (top) and pCHK036 (bottom) with pLVPK (middle). The locations of the genes on the plasmid circle map are indicated. Genes in blue, Orange, red and purple represent the drug resistance genes, mobile elements, virulence genes and other genes, respectively. The intermediate gray area represents genes blast homology.

with the paradigm virulence plasmid pLVPK (accession numbers NC_005249.1). BLASTn query revealed that pCHK014 shared a higher identity (99.92%) with pLVPK compared to pCHK036-1 (95.92%) even though they both had low coverage (36% and 21%, respectively) aligned to pLVPK as pLVPK-derived CG43 strain belong to ST86 rather than ST25, suggesting that the virulence plasmid of hvKp CHK014 had higher evolutionary conservations with hypervirulent pLVPK than that of non-hvKp CHK036 in core virulence gene islands (Figure 4).

The *rmp* homologues are associated with CPS biosynthesis. Given the difference in hypermucoviscosity observed between hvKp CHK014 and non-hvKp CHK036 in the string test (Table 1), and the upregulated expression of *rmpA*. Compared to NTUH-K2044 chromosomes, c-RmpA gene on CHK036 had no variant, but c-RmpD had 2 missenses, and c-RmpC had 1 missense. Compared to pLVPK, c-RmpA amino acid sequence on CHK036 showed 19 missenses, whereas p-RmpA on CHK014 showed totally the same amino acid sequences with pLVPK. Furthermore, we examined the promoter region between −1 and −300 bp upstream of the transcription start site (TSS) of *rmpA* in both isolated strains, comparing them with that in pLVPK. The promoter region of plasmid-*rmpA* (p-*rmpA*) on CHK014 was conserved, while the same region of chromosomal *rmpA* (c-*rmpA*) on CHK036 displayed 38 variants (including 34 SNPs, 2 deletions and 2 insertions). Besides, compared to NTUH-K2044 c-*rmpA*, CHK036 c-*rmpA* demonstrated 1 deletion at −196 bp position upstream of the TSS.

Interestingly, we also noted a difference in the poly(T) track of the *rmpA* promoter between the −77 and −45 sites as recently reported by Liu et al.[28] A poly(T) track with 11 consecutive thymine residues (P_{11T}), a characteristic feature of the active *rmpA* promoter in pLVPK, was identified in hvKp CHK014. In contrast, non-hvKp CHK036 exhibited a truncated poly(T) track with 10 thymine residues (P_{10T}) in the *rmpA* promoter region (Figure 5).

Discussion

An outbreak of K2-ST25 hvKp, a subclone distinct from the more common K1-ST23 and K2-ST86/ST65/ST375 hvKp clones,[4,5] was observed in the neonatal unit. Previous research on pediatric hvKp surveillance revealed that K1 and K2 capsules were the most prevalent hvKp genotypes,[16] with K1-ST23 and novel clones like K2-ST25 and K19-ST660 being particularly common. Notably, K2-ST25 *K. pneumoniae* also caused an outbreak among adult patients in another

https://doi.org/10.2147/IDR.S573797

Figure 5 Sequence alignment of distinct *rmpA* promoters from pLVPK, CHK014 and CHK036. Based on the poly (T) track, "P_{11T}" was marked red and "P_{10T}" was marked blue.

single center in China.[7,29] Therefore, it is crucial to monitor and implement necessary measures to prevent the dissemination and infections of these clonal hvKp strains, including K2-ST25, in both clinical and community settings. Identifying neonatal patients who matched the epidemiological profiles to the isolates could assist in interventions to prevent or promptly manage hvKp infections.

In the comparative analysis, we investigated two K2-ST25 strains, hvKp CHK014 and non-hvKp CHK036. Our findings revealed that virulence-associated genes *rmpA, peg344*, and the *iro* operon were located in ICE*Kp1* on the chromosome in CHK036, whereas in CHK014, these genes were situated on the nonconjugative IncFIB/IncHI3B virulence plasmid. CPS was a crucial virulence determinant, with isogenic non-capsulated strains showing reduced pathogenicity in murine infection models when compared to capsulated strains.[30] Phenotypical assays demonstrated that CHK014 exhibited significantly higher CPS yields, a trait previously reported to be regulated by the *rmpA* gene,[2] compared to CHK036. Furthermore, RT-qPCR analysis revealed significantly elevated expression levels of the *rmpA* gene in CHK014 as opposed to CHK036. Interestingly, CHK014 carrying the p-*rmpA* showed positive in the string test, while CHK036 with the c-*rmpA* showed negative. For typical hvKP such as NTUH-K2044, Hsu CR et al believed that the *rmpA* on the large plasmid (p-*rmpA*) not the *rmpA* on the chromosome (c-*rmpA*) upregulated CPS synthesis and virulence,[31] and several studies supported significant increases in the 50% lethal dose in intraperitoneal models for K2 type p-*rmpA* mutants strain compared to the isogenic K2 hypermucoviscous wild-type.[2,32] Furthermore, we focused on the possibility of heterogeneous *rmpA* promoters that influenced its expression and might lead to the virulence divergence of K2-ST25 *K. pneumoniae*. Notably, *rmpA* promotor in hvKP CHK014 exhibited greater similarity to pLVPK than that in non-hvKp CHK036. Additionally, we discovered the polymorphism in the poly(T) region upstream of the TSS of *rmpA* gene between CHK036 and CHK014, which probably contributed to their differing virulence profile as previously reported by Liu et al.[28] The study by Liu et al[28] primarily focused on K64-ST11 carbapenem-resistant hypervirulent *K. pneumoniae* (CR-hvKp), whereas our research extends these findings to K2-ST25 hvKp, providing further insights into the molecular mechanism underlying hypervirulence.

Interestingly, hvKP CHK014 exhibited brighter orange halos than non-hvKP CHK036 on siderophore plates in the qualitative plate assay, despite CHK014 demonstrated a significant decrease in siderophore production compared to CHK036 in the quantitative siderophore production assay, both of two strains exhibited orange halos (Figure 3D and E). Since the *iuc* and *iro* lineages were siderophores determinants,[2,3] the absence of *iuc* lineage in CHK014 substantially affected the siderophore production, in spite of the higher expression of *iroB* in CHK014 than in CHK036. Recently, some studies revealed that PEG344, an inner membrane transporter, was required for full virulence of hvKP after pulmonary but not subcutaneous challenge,[27] in our study, hvKP CHK014 had higher expression of *peg344* than non-hvKP CHK036 (Figure 3F) and CHK014 - intraperitoneally infected mice had higher mortality, which needs further investigation on virulence of PEG344 factor in the murine intraperitoneal infection model. As hvKP 2019K134 and CHK014 infection cause significantly more damage (shorter median lethal time, more bacterial burden and more bleeding) in mice than non-hvKP CHK036, the method distinguished hvKp and non-hvKP with virulence-associated genes isolates in our previous study was considered feasible.[16] Thus, even K2-ST25 non-hvKP carried *iuc* and *iro* lineages and produced much more siderophores (Table 1), we attribute hypervirulence of hvKP isolates to the expression level of *rmpA* gene.

Nearly three-quarters of hvKp[33] and 90% of CG23 strains harbored ICEs.[34] Among these, ICE*Kp1* often carried the *rmpA* and *iro* genes.[35] In our study, the *rmpA* gene, together with the *iroD-iroC-iroB-iroN* operon, *iutA* gene and *peg344* gene, in the non-hvKp CHK036 strain was found to be located on the conjugative chromosomal ICE*Kp1*. This arrangement might facilitate the transfer of these virulence genes to CRKP, leading to the formation of CR-hvKp. The ICE*Kp1* was adjacent to the *asn* tRNA gene, flanked by 15-bp direct repeats on both sides.[36] However, the order of the *iro* genes within the operon was different from the typical ICE*Kp1*.

Besides the chromosomal *rmpA, iutA, peg344* and *iro* genes in the mobile elements, CHK036 also harbored the plasmid-encoded *iucABCD-iutA* virulence gene cluster. This cluster was located within the IncFIB/IncFII conjugative virulence plasmid pCHK036-1, which likely underwent horizontal transfer but no longer retains its virulence. As plasmids could be energetically costly due to the need for extra DNA replication and expression, potentially leading to mutations in both plasmids, and chromosome to enhance host fitness,[37] thus it was plausible that the presence of plasmids could impact the expression of the chromosomal *rmpA* gene in CHK036. This hypothesis was supported by the higher mutation rate in its promoter region in CHK036 strain.

Recent findings have uncovered the involvement of multiple regulators, such as *KvrA, KvrB*, and *RcsB*, in controlling *rmpA* expression, expanding beyond capsule regulation.[38] Only a small portion of the genes carried by virulence plasmids had been characterized so far,[3] and this study focused solely on key virulence genes like *rmpA, rmpA2, iuc*, and *iro*, but we showed unique gene families in the hvKp CHK014 distinguishing from non-hvKp CHK036 through GO and KEGG analysis (Figure S1 and Table S3), which were potential unidentified genetic biomarkers differentiating hvKp from cKP.

Conclusions

In our study, we observed an outbreak of K2-ST25 hvKP in the neonatal unit, among which two strains demonstrated difference in virulence using a murine infection model. WGS data revealed that the *rmpA* gene of the non-hvKp strain CHK036 was located in ICE*Kp1* on the chromosome, while the *rmpA* gene of the hvKp strain CHK014 was located in the virulence plasmid. Furthermore, RT-qPCR and in vitro CPS production assay showed that the expression level of the plasmid-*rmpA* gene in CHK014 was significantly higher than that of the chromosomal *rmpA* gene in CHK036. The association between the poly(T) variants and the virulence was recently reported in K64-ST11 CR-hvKp, our study indicated the functional feature of this cis-element was shared within a broad spectrum of hvKp subtypes. Nonetheless, corresponding regulatory mechanisms involving transcription factors were still required further investigation.

Data Sharing Statement

The data that support the findings of this study have been deposited with the National Center for Biotechnology Information (NCBI) under Bioproject PRJNA1015570.

Acknowledgments

The authors gratefully acknowledge all members of the Clinical Laboratory of Shanghai Children's Hospital for their cooperation and technical help.

Funding

This work was supported by Shanghai Municipal Key Clinical Specialty (shslczdzk06902), the Natural Science Foundation of Shanghai (21ZR1452900), Municipal Commission of Health and Family Planning (201940253), Shanghai "Rising Stars of Medical Talents" Youth Development Program (Youth Medical Talents –Clinical Laboratory Practitioner Program), research project of Shanghai Children's Hospital (2020YGZQ06), and Three-Year Initiative Plan for Strengthening Public Health System Construction in Shanghai (2023–2025) (GWVI-3).

Disclosure

The authors report no conflicts of interest in this work.

References

1. Fang CT, Chuang Y-P, Shun C-T, et al. A novel virulence gene in *Klebsiella pneumoniae* strains causing primary liver abscess and septic metastatic complications. *J Exp Med*. 2004;199(5):697–705. doi:10.1084/jem.20030857
2. Cheng HY, Chen YS, Wu CY, et al. RmpA regulation of capsular polysaccharide biosynthesis in *Klebsiella pneumoniae* CG43. *J Bacteriol*. 2010;192(12):3144–3158. doi:10.1128/JB.00031-10
3. Chen YT, Chang H-Y, Lai Y-C, et al. Sequencing and analysis of the large virulence plasmid pLVPK of *Klebsiella pneumoniae* CG43. *Gene*. 2004;337:189–198. doi:10.1016/j.gene.2004.05.008
4. Shon AS, Bajwa RP, Russo TA. Hypervirulent (hypermucoviscous) *Klebsiella pneumoniae*: a new and dangerous breed. *Virulence*. 2013;4 (2):107–118. doi:10.4161/viru.22718
5. Lee CR, Lee JH, Park KS, et al. Antimicrobial resistance of hypervirulent *Klebsiella pneumoniae*: epidemiology, hypervirulence-associated determinants, and resistance mechanisms. *Front Cell Infect Microbiol*. 2017;7:483. doi:10.3389/fcimb.2017.00483
6. Cejas D, Elena A, Guevara Nuñez D, et al. Changing epidemiology of KPC-producing *Klebsiella pneumoniae* in Argentina: emergence of hypermucoviscous ST25 and high-risk clone ST307. *J Glob Antimicrob Resist*. 2019;18:238–242. doi:10.1016/j.jgar.2019.06.005
7. Li J, Huang Z-Y, Yu T, et al. Isolation and characterization of a sequence type 25 carbapenem-resistant hypervirulent *Klebsiella pneumoniae* from the mid-south region of China. *BMC Microbiol*. 2019;19(1):219. doi:10.1186/s12866-019-1593-5
8. Holt KE, Wertheim H, Zadoks RN, et al. Genomic analysis of diversity, population structure, virulence, and antimicrobial resistance in *Klebsiella pneumoniae*, an urgent threat to public health. *Proc Natl Acad Sci U S A*. 2015;112(27):E3574–81. doi:10.1073/pnas.1501049112
9. Lin J, Huang Y, Qian L, et al. Liver abscess combined with endogenous endophthalmitis caused by genotype ST25 serotype K2 hypervirulent *Klebsiella pneumoniae*: a case report. *Infect Drug Resist*. 2022;15:4557–4561. doi:10.2147/IDR.S376443
10. Collins AM, Mizzi R. Virulence determinants in *Klebsiella pneumoniae* associated with septicaemia outbreaks in neonatal pigs. *Vet Microbiol*. 2025;302:110409. doi:10.1016/j.vetmic.2025.110409
11. Naing SY, Zomer A, der Graaf-van Bloois LV, et al. Molecular epidemiology and emergence of sequence type 25 hypervirulent *Klebsiella pneumoniae* in pigs in the Netherlands (2013-2020): a global comparative analysis with human and pig isolates. *Microb Genom*. 2025;11(4).
12. Xia P, Yi M, Yuan Y, et al. Coexistence of multidrug resistance and virulence in a single conjugative plasmid from a hypervirulent *Klebsiella pneumoniae* isolate of sequence type 25. *Msphere*. 2022;7(6):e0047722. doi:10.1128/msphere.00477-22
13. Veloso M, Arros P, Acosta J, et al. Antimicrobial resistance, pathogenic potential, and genomic features of carbapenem-resistant *Klebsiella pneumoniae* isolated in Chile: high-risk ST25 clones and novel mobile elements. *Microbiol Spectr*. 2023;11(5):e0039923. doi:10.1128/spectrum.00399-23
14. Albarracin L, Ortiz Moyano R, Vargas JM, et al. Genomic and immunological characterization of hypermucoviscous carbapenem-resistant *Klebsiella pneumoniae* ST25 isolates from Northwest Argentina. *Int J Mol Sci*. 2022;23(13):7361. doi:10.3390/ijms23137361
15. Russo TA, Olson R, Fang C-T, et al. Identification of biomarkers for differentiation of hypervirulent *Klebsiella pneumoniae* from Classical *K. pneumoniae*. *J Clin Microbiol*. 2018;56(9). doi:10.1128/JCM.00776-18
16. Du Q, Pan F, Wang C, et al. Nosocomial dissemination of hypervirulent *Klebsiella pneumoniae* with high-risk clones among children in Shanghai. *Front Cell Infect Microbiol*. 2022;12:984180. doi:10.3389/fcimb.2022.984180
17. CLSI. Performance standards for antimicrobial susceptibility testing. 31st ed. CLSI supplement M100. *Clinical and Laboratory Standards Institute*. 2021.
18. CDER. Tygacil® (tigecycline) for injection. Application number 21-821. Center for Drug Evaluation and Research. 2005.
19. Tsuji BT, Pogue JM, Zavascki AP, et al. International consensus guidelines for the optimal use of the polymyxins: endorsed by the American College of Clinical Pharmacy (ACCP), European Society of Clinical Microbiology and Infectious Diseases (ESCMID), Infectious Diseases Society of America (IDSA), International Society for Anti-infective Pharmacology (ISAP), Society of Critical Care Medicine (SCCM), and Society of Infectious Diseases Pharmacists (SIDP). *Pharmacotherapy*. 2019;39(1):10–39. doi:10.1002/phar.2209
20. Magiorakos AP, Srinivasan A, Carey RB, et al. Multidrug-resistant, extensively drug-resistant and pandrug-resistant bacteria: an international expert proposal for interim standard definitions for acquired resistance. *Clin Microbiol Infect*. 2012;18(3):268–281. doi:10.1111/j.1469-0691.2011.03570.x
21. Kuo HY, Chang K-C, Kuo J-W, et al. Imipenem: a potent inducer of multidrug resistance in Acinetobacter baumannii. *Int J Antimicrob Agents*. 2012;39(1):33–38. doi:10.1016/j.ijantimicag.2011.08.016
22. Livak KJ, Schmittgen TD. Analysis of relative gene expression data using real-time quantitative PCR and the 2(-Delta Delta C(T)) method. *Methods*. 2001;25(4):402–408. doi:10.1006/meth.2001.1262
23. Zhang Y, Jin L, Ouyang P, et al. Evolution of hypervirulence in carbapenem-resistant *Klebsiella pneumoniae* in China: a multicentre, molecular epidemiological analysis. *J Antimicrob Chemother*. 2020;75(2):327–336. doi:10.1093/jac/dkz446
24. Wang B, Pan F, Han D, et al. Genetic characteristics and microbiological profile of hypermucoviscous multidrug-resistant Klebsiella variicola coproducing IMP-4 and NDM-1 carbapenemases. *Microbiol Spectr*. 2022;10(1):e0158121. doi:10.1128/spectrum.01581-21
25. Mike LA, Stark AJ, Forsyth VS, et al. A systematic analysis of hypermucoviscosity and capsule reveals distinct and overlapping genes that impact *Klebsiella pneumoniae* fitness. *PLoS Pathog*. 2021;17(3):e1009376. doi:10.1371/journal.ppat.1009376
26. Wang J, Ma R, Pan F, et al. The molecular epidemiology of prevalent *Klebsiella pneumoniae* strains and humoral antibody responses against carbapenem-resistant *K. pneumoniae* infections among pediatric patients in Shanghai. *Msphere*. 2022;7(5):e0027122. doi:10.1128/msphere.00271-22
27. Bulger J, MacDonald U, Olson R, et al. Metabolite transporter PEG344 is required for full virulence of hypervirulent *Klebsiella pneumoniae* strain hvKP1 after pulmonary but not subcutaneous challenge. *Infect Immun*. 2017;85(10). doi:10.1128/IAI.00093-17
28. Liu L, Lou N, Liang Q, et al. Chasing the landscape for intrahospital transmission and evolution of hypervirulent carbapenem-resistant *Klebsiella pneumoniae*. *Sci Bull*. 2023;68(23):3027–3047. doi:10.1016/j.scib.2023.10.038
29. Yao B, Xiao X, Wang F, et al. Clinical and molecular characteristics of multi-clone carbapenem-resistant hypervirulent (hypermucoviscous) *Klebsiella pneumoniae* isolates in a tertiary hospital in Beijing, China. *Int J Infect Dis*. 2015;37:107–112. doi:10.1016/j.ijid.2015.06.023

30. Cortés G, Borrell N, de Astorza B, et al. Molecular analysis of the contribution of the capsular polysaccharide and the lipopolysaccharide o side chain to the virulence of *Klebsiella pneumoniae* in a murine model of pneumonia. *Infect Immun*. 2002;70(5):2583–2590. doi:10.1128/IAI.70.5.2583-2590.2002
31. Hsu CR, Lin T-L, Chen Y-C, et al. The role of *Klebsiella pneumoniae* rmpA in capsular polysaccharide synthesis and virulence revisited. *Microbiology*. 2011;157(Pt 12):3446–3457. doi:10.1099/mic.0.050336-0
32. Nassif X, Fournier JM, Arondel J, et al. Mucoid phenotype of *Klebsiella pneumoniae* is a plasmid-encoded virulence factor. *Infect Immun*. 1989;57(2):546–552. doi:10.1128/iai.57.2.546-552.1989
33. Marcoleta AE, Berríos-Pastén C, Nuñez G, et al. *Klebsiella pneumoniae* asparagine tDNAs are integration hotspots for different genomic islands encoding microcin E492 production determinants and other putative virulence factors present in hypervirulent strains. *Front Microbiol*. 2016;7:849. doi:10.3389/fmicb.2016.00849
34. Lam MMC, Wyres KL, Duchêne S, et al. Population genomics of hypervirulent *Klebsiella pneumoniae* clonal-group 23 reveals early emergence and rapid global dissemination. *Nat Commun*. 2018;9(1):2703. doi:10.1038/s41467-018-05114-7
35. Lin TL, Lee C-Z, Hsieh P-F, et al. Characterization of integrative and conjugative element ICE Kp1 -associated genomic heterogeneity in a *Klebsiella pneumoniae* strain isolated from a primary liver abscess. *J Bacteriol*. 2008;190(2):515–526. doi:10.1128/JB.01219-07
36. Yang X, Ye L, Li Y, et al. Identification of a chromosomal integrated DNA FRAGMENT CONTAINING the rmpA2 and iucABCDiutA virulence genes in *Klebsiella pneumoniae*. *Msphere*. 2020;5(6). doi:10.1128/mSphere.01179-20
37. Gama JA, Zilhão R, Dionisio F. Impact of plasmid interactions with the chromosome and other plasmids on the spread of antibiotic resistance. *Plasmid*. 2018;99:82–88. doi:10.1016/j.plasmid.2018.09.009
38. Walker KA, Miner TA, Palacios M, et al. A *Klebsiella pneumoniae* regulatory mutant has reduced capsule expression but retains hypermucoviscosity. *mBio*. 2019;10(2). doi:10.1128/mBio.00089-19